LANGMUIR

Extension of the SAFT-VR Mie EoS To Model Homonuclear Rings and Its Parametrization Based on the Principle of Corresponding States

Erich A. Müller[†][ID] and Andrés Mejía*[,‡][ID]

[†]Department of Chemical Engineering, Imperial College London, South Kensington Campus, London SW7 2AZ, United Kingdom
[‡]Departamento de Ingeniería Química, Universidad de Concepción POB 160 − C, Correo 3, Concepción, Chile

[S] *Supporting Information*

ABSTRACT: The statistical associating fluid theory of variable range employing a Mie potential (SAFT-VR-Mie) proposed by Lafitte et al. (*J. Chem Phys.* **2013**, *139*, 154504) is one of the latest versions of the SAFT family. This particular version has been shown to have a remarkable capability to connect experimental determinations, theoretical calculations, and molecular simulations results. However, the theoretical development restricts the model to chains of beads connected in a linear fashion. In this work, the capabilities of the SAFT-VR Mie equation of state for modeling phase equilibria are extended for the case of planar ring compounds. This modification proposed replaces the Helmholtz energy of chain formation by an empirical contribution based on a parallelism to the second-order thermodynamic perturbation theory for hard sphere trimers. The proposed expression is given in terms of an extra parameter, χ, that depends on the number of beads, m_s, and the geometry of the ring. The model is used to describe the phase equilibrium for planar ring compounds formed of Mie isotropic segments for the cases of m_s equals to 3, 4, 5 (two configurations), and 7 (two configurations). The resulting molecular model is further parametrized, invoking a corresponding states principle resulting in sets of parameters that can be used indistinctively in theoretical calculations or in molecular simulations without any further refinements. The extent and performance of the methodology has been exemplified by predicting the phase equilibria and vapor pressure curves for aromatic hydrocarbons (benzene, hexafluorobenzene, toluene), heterocyclic molecules (2,5-dimethylfuran, sulfolane, tetrahydro-2*H*-pyran, tetrahydrofuran), and polycyclic aromatic hydrocarbons (naphthalene, pyrene, anthracene, pentacene, and coronene). An important aspect of the theory is that the parameters of the model can be used directly in molecular dynamics (MD) simulations to calculate equilibrium phase properties and interfacial tensions with an accuracy that rivals other coarse grained and united atom models, for example, liquid densities, are predicted, with a maximum absolute average deviation of 3% from both the theory and the MD simulations, while the interfacial tension is predicted, with a maximum absolute average of 8%. The extension to mixtures is exemplified by considering a binary system of hexane (chain fluid) and tetrahydro-2*H*-pyran (ring fluid).
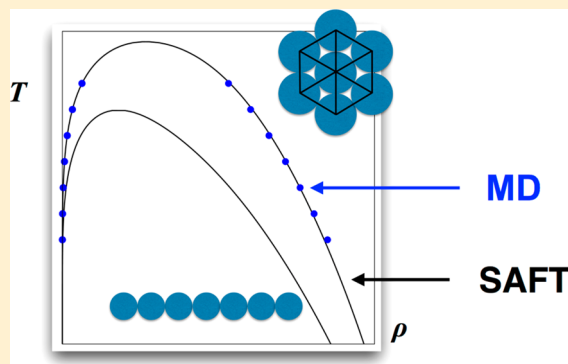
INTRODUCTION

The Statistical Associating Fluid Theory (SAFT) equation of state (EoS) is one of the most versatile, advanced, and accurate molecular-based EoS used to predict the thermophysical properties of pure fluids and fluid mixtures. Its formulation is based on Wertheim's first-order thermodynamic perturbation theory (TPT1)[1−4] and expressed as a sum of contributions to the Helmholtz free energy, namely:

$$a = a^{IG} + a^{MONO} + a^{CHAIN} + a^{ASSOC} \qquad (1)$$

where a is the dimensionless Helmholtz energy, defined as $a = A/(Nk_BT)$; A being the total Helmholtz energy, N the number of molecules, k_B the Boltzmann constant, and T the temperature. a^{IG} is the ideal gas reference value, while the other terms correspond to increased complexity in the model; a^{MONO} adds the monomer (unbounded) contribution for a chain composed of m_s tangential segments, a^{CHAIN} accounts for

the formation of said chains, while a^{ASSOC} is the Helmholtz energy contribution accounting for intermolecular association. Since its inception within the Gubbins group in the late 80s, several variants of the SAFT EoS have been proposed in order to incrementally improve its accuracy and range of applicability. It is arguably one of the most important advances in the area of correlation and prediction of fluid phase properties of the last decades. For an abridged overview of the SAFT EoS and its most recent versions, the reader is directed to the available reviews in the open literature.[5−9] Without prejudice to other

implementations, the SAFT-VR Mie proposed by Lafitte et al.[10] is employed here, as it provides a remarkable route to connect experimental determinations, theoretical calculations, and molecular simulations results.[11] Its success is attributed to two factors, the versatility of the underlying potential and its accuracy in representing said potential. The Mie potential,[12] ϕ_{Mie},

$$\phi_{\text{Mie}}(r) = \left(\frac{\lambda_r}{\lambda_r - \lambda_a}\right)\left(\frac{\lambda_r}{\lambda_a}\right)^{\lambda_a/(\lambda_r - \lambda_a)} \varepsilon\left[\left(\frac{\sigma}{r}\right)^{\lambda_r} - \left(\frac{\sigma}{r}\right)^{\lambda_a}\right]$$

(2)

where r is the distance between centers of the particles, ε is the minimum energy of interaction, σ is the short distance where the repulsive and attractive contribution of the potential cancel and λ_r and λ_a are the exponents that characterize ultimate range of the interaction. It represents an "upgrade" of the commonly used Lennard-Jones ($\lambda_r = 12$; $\lambda_a = 6$), incorporating a flexibility in the treatment of the attractive range and repulsive nature of the intermolecular potential, whereas the inclusion of a perturbation expansion of the underlying monomer term, a^{MONO}, to third order allows the theory to describe with precision the expected macroscopic behavior of the potential. This latter aspect is particularly important, as it allows the exploitation of the link between the theoretical description by means of an EoS and the direct molecular simulation of the corresponding fluid. The accuracy of this one-to-one correspondence is crucial in order to represent molecules as coarse-grained (CG) beads with molecular parameters provided by the fitting of the SAFT model to experimental data.[13] The procedure essentially defines a top-down coarse grained approach that has been widely successful in modeling both the phase equilibria, interfacial properties, and self-assembly of organic molecules, polymers, surfactants, and mixtures.[14−19]

In one of the seminal manuscripts defining the above theory, Lafitte et al.,[16] recognized the importance of having the appropriate overall shape of the molecular model. TPT1, on which most of the SAFT formulations are based on, adds to the monomer term of the Helmholtz energy an explicit contribution corresponding to the free energy required to form a chain from the corresponding monomer segments. While TPT1 makes no explicit provision for the connectivity of the beads, an analysis of the assumptions made in the theory with regards to the three (and higher body) distribution functions immediately suggests that the theory will be most accurate for linear chains (or completely flexible and extended chains).[20] Molecules formed by beads connecting each other in a nonlinear fashion require a fundamentally different approach, essentially invoking Wertheim's second order perturbation theory (TPT2).[21] If one is to consider phase equilibria applications, whereas the parameters of the EoS are fitted to experimental data, and the resulting analytical expression is used to correlate and extrapolate the bulk thermodynamic properties, the nuances of the shape of the molecule and those of the underlying potential are to a great extent irrelevant. As a consequence of that the various versions of SAFT (and indeed of any other modern EoS) fundamentally provide comparable accuracy among themselves, and all serve as appropriate tools for use in engineering and spreadsheet calculations.[9] A key point raised by Lafitte et al.,[16] is that the shape of the underlying molecular model, while having modest effect on the bulk thermodynamic properties, has an important role in the accurate description of the structure of the fluid, as probed by

molecular simulation. In ref 16, tasked with the challenge of representing a discotic molecule like benzene as a ring of three beads bonded to form an equilateral triangle, it was suggested to replace the a^{CHAIN} term in the SAFT-VR Mie EoS (see eq 1) by an empirical a^{RING} term proposed by Sear and Jackson.[22] The performance of this new model was tested by comparing the phase equilibria (i.e., temperature−density coexistence envelope and Clausius−Clapeyron curve) and interfacial tension results for benzene to alternative models such as a single-segment CG sphere, a geometrically accurate six-segment TraPPE United Atom[23] model and available experimental data. As concluded in ref 16, the three-segment CG ring is an excellent approximation displaying good agreement with experiments for subcritical and critical phase equilibria, interfacial tension, and as an ancillary benefit avoids the premature freezing exhibited by the single bead model. More importantly, however, the ring model displays the correct behavior for the fluid structure, as evidenced by the center of mass pair distribution function. The Lafitte et al.,[16] approach suffers from two drawbacks: the accuracy with which the Sear and Jackson a^{RING} term represents the potential is limited (hence the need to rescale the EoS parameters when attempting to employ them in simulations) and the absence of information on the actual ring geometry. The latter limitation is particularly important for the case of ring components with more than three segments. In principle, an expression for ring molecules can be obtained by taking the limit of an associating fluid that can either self-associate (as a snake biting its tail) or associate forming rings. This latter approach is discussed recently by Haghmoradi et al.[24] and the reader is referred to said manuscript for a review of the existing alternative approaches.
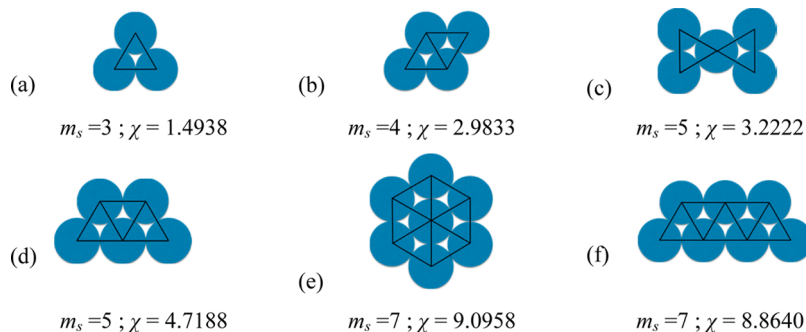
This work reports a revised expression for the a^{RING} term of the SAFT-VR Mie EoS that allows the parameters to be used within molecular simulations. The proposed model is developed with input from TPT2, adapted and informed by molecular simulations of models of ring molecules. The resulting model is further parametrized, employing a corresponding states correlation, to establish a link between the force field parameters and a selected set of macroscopical properties.

Helmholtz Energy for Rings. The TPT1 theory, upon which SAFT is based, "forbids" the combination of monomers in such a way that a closed ring (or a branched chain) is formed. In spite of this limitation, versions of the SAFT EoS have been used to model rings compounds, by employing the molecular chain length (m_s) as a lumped parameter that absorbs the geometric shape of molecule. An example of this approach was presented by Huang and Radosz,[25] where correlations for the parameters of polynuclear aromatic compounds (PAH) are presented in terms of molecular weights. In this (and similar approaches), the molecular parameters used for these compounds can not be transferred to molecular simulations and, in general, the corresponding values of the chain length m_s do not provide any physical link to the actual molecular geometry.

A closer look at the perturbation form of the SAFT EoS reveals that the contribution to the Helmholtz energy of forming a ring structure must be encapsulated in the a^{CHAIN} term of eq 1, which has the general form of

$$a^{\text{CHAIN}} = -C \ln[g^{\text{ref}}(\sigma)]$$

(3)

where $g_{\text{ref}}(\sigma)$ denotes the contact value of the radial pair distribution function for the reference monomeric fluid. Sear

Table 1. Ring Molecule Geometries and Values for the Parameter χ (Eq 5)[a]

| (a) $m_s = 3$; $\chi = 1.4938$ | (b) $m_s = 4$; $\chi = 2.9833$ | (c) $m_s = 5$; $\chi = 3.2222$ |
| (d) $m_s = 5$; $\chi = 4.7188$ | (e) $m_s = 7$; $\chi = 9.0958$ | (f) $m_s = 7$; $\chi = 8.8640$ |

[a]All molecular models are planar, built from m_s tangent Mie spheres, bonded rigidly at a distance σ from the center of adjacent beads. The lines between the centers of neighbouring beads form equilateral triangles.
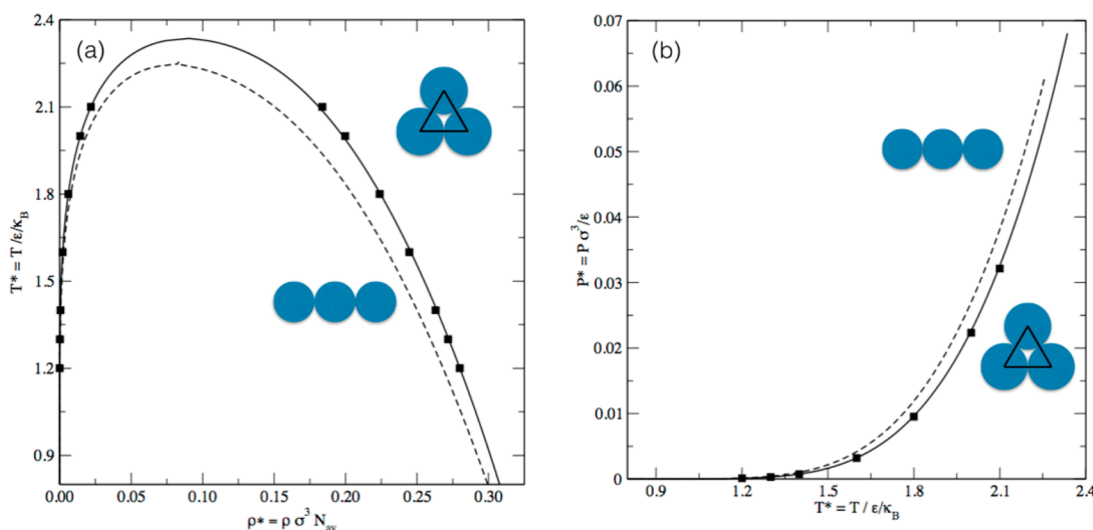

Figure 1. Phase equilibrium for $m_s = 3$: (a) coexistence densities ($\rho-T$ projection), (b) vapor pressure ($T-P$ projection); (■) MD results; (—) SAFT-VR Mie EoS calculations with $\chi = 1.4938$ (ring fluid); (- - -) SAFT-VR Mie EoS calculations with $\chi = 0$ (chain fluid).

and Jackson[22,26,27] proposed that if within TPT1 C can be loosely interpreted as the contribution to form $(m_s - 1)$ covalent-like bonds between m_s monomers and takes the form of $C = (m_s - 1)$ for a linear chain, then for the case of an m_s-membered ring of tangential segments, the expression for the Helmholtz energy for rings (a^{RING}) should be given by eq 3 with $C = m_s$. The background for this ansatz is that in the case of a circular structure an "additional" bond is being made between the first and last member of a chain to form the ring structure. The use of this closure does not always give satisfactory results: the results of Lafitte et al.[16] suggested that the EoS parameters obtained when using this ansatz and fitting experimental data of vapor pressure and liquid density, need to be rescaled in order to be further used in molecular simulations. The fact that the linear version of the theory does not require such scaling implies some degree of inconsistency.

Müller and Gubbins[20] explored the extension of TPT1 to second order (TPT2) and obtained rigorous expressions for the EoS for molecular geometries of rings of $m_s = 3$ for hard fluids. These expressions are based on the knowledge of the three-body distribution functions of the hard sphere reference fluid and depend on the density (packing fraction) of the system. One can compare analytically the results of a linear chain of three beads with that of a ring of three beads and extract from the comparison the "equivalent" value of C to be used within

TPT1 to accurately represent a ring. Further details are supplied in the Appendix, but it suffices to say that the derivation leads expression for C with the following form

$$C = m_s - 1 + \chi\eta \tag{4}$$

where η is the packing fraction, $\eta = m_s\pi\rho\sigma^3/6$, ρ is the molecular number density, and χ is a parameter which depends on the geometry and the reference potential. It is noteworthy that for $\chi = 0$, the usual TPT1 expression for linear chains is recovered. While $\chi = 1.3827$ is an exact result for a hard sphere system of triangles (see Appendix), in order to employ a similar approach for other geometrical realizations of planar rings, we postulate the following general form for the contribution to ring formation for the SAFT-VR Mie EoS

$$a^{\mathrm{RING}} = -C \ln[g^{\mathrm{Mie}}(\sigma)] = -(m_s - 1 + \chi\eta)\ln[g^{\mathrm{Mie}}(\sigma)] \tag{5}$$

where χ is defined as a parameter, function of m_s and the actual geometrical connection of the ring. For chain fluids of $m_s > 3$, and soft potentials TPT2 is not fully developed and analytical expressions are not available, hence, the procedure outlined above for hard triangles is not applicable. For the same reason, for soft potentials, the packing fraction is ill-defined and reverts essentially to a measure of the system density. We seek to exploit the correspondence between the SAFT-VR Mie EoS
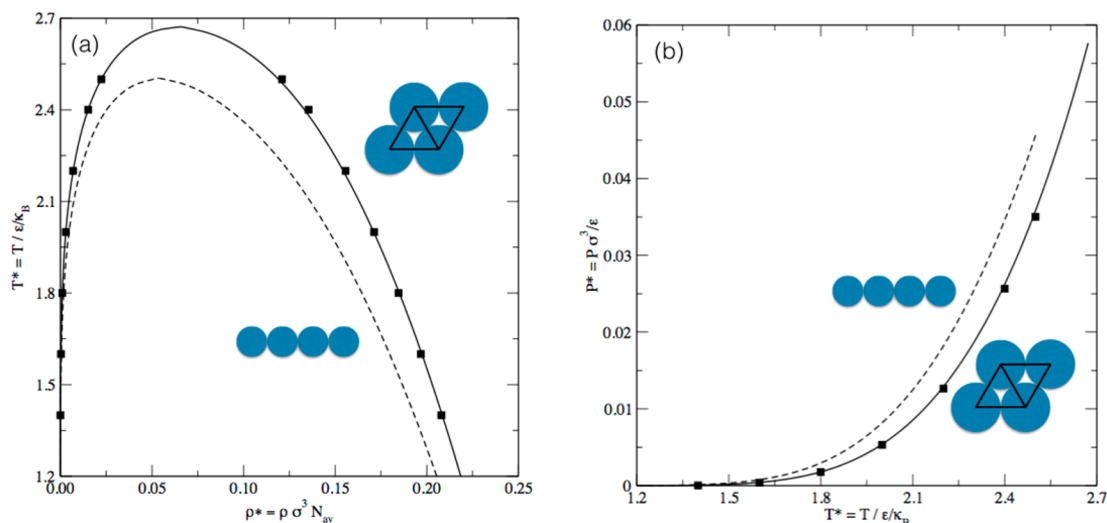
Figure 2. Phase equilibrium for $m_s = 4$: (a) coexistence densities ($\rho-T$ projection), (b) vapor pressure ($T-P$ projection); (■) MD results; (—) SAFT-VR Mie EoS calculations with $\chi = 2.9833$; (- - -) SAFT-VR Mie EoS calculations with $\chi = 0$ (chain fluid).
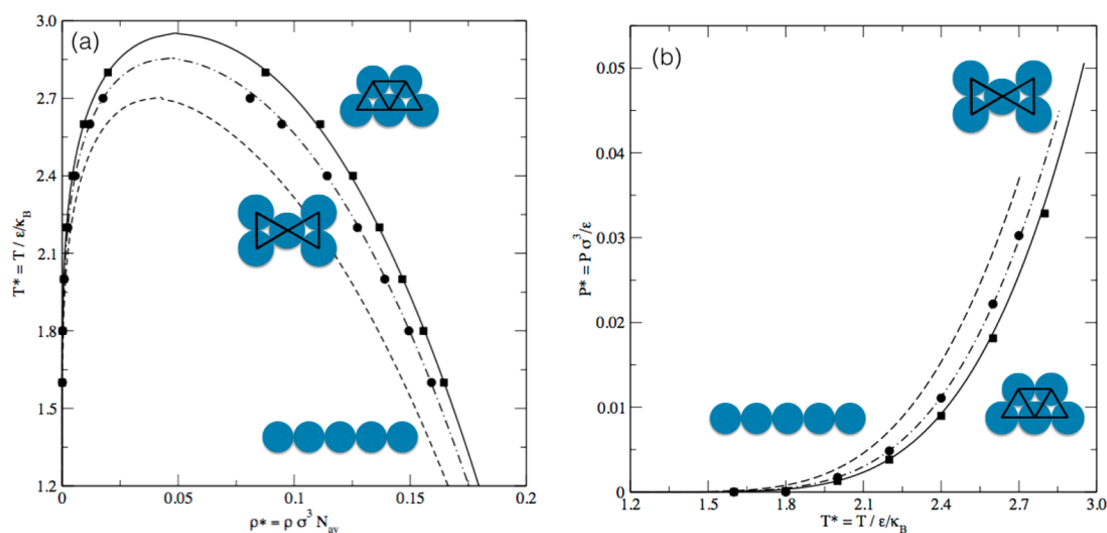

Figure 3. Phase equilibrium for $m_s = 5$: (a) coexistence densities ($\rho-T$ projection), (b) vapor pressure ($T-P$ projection); (■) MD results for geometry (d) from Table 1; (●) MD results for geometry (c) from Table 1; (—) SAFT-VR Mie EoS calculations with $\chi = 4.7188$ (geometry (d) from Table 1); (— · —) SAFT-VR Mie EoS calculations with $\chi = 3.2222$ (geometry (c) from Table 1); (- - -) SAFT-VR Mie EoS calculations with $\chi = 0$ (chain fluid).

and the underlying Mie potential and employ Canonical (NVT) molecular dynamics (MD) simulations carried out for a defined pure fluid (i.e., fixed geometry and molecular parameters: m_s, ε, σ, λ_r, λ_a) and use them as pseudoexperimental data to calculate χ from the EoS. We explored the phase equilibrium behavior of planar pure ring fluids for the cases of $m_s = 3$, $m_s = 4$, $m_s = 5$ (two configurations), and $m_s = 7$ (two configurations). While we use a single set of molecular parameters: $\varepsilon/k_B = 250$ K, $\sigma = 3.0$ Å, $\lambda_r = 11.0$ and $\lambda_a = 6.0$ for the simulations, we will later extend these results employing a corresponding states principle. Simulation details and numerical values of the simulations are given as part of the Supporting Information. In Table 1, we summarize the resulting values of χ along with the graphical representation of the ring geometries used.

Figures 1−4 illustrate the phase equilibrium ($\rho-T$ projection) and vapor pressure diagram ($T-P$ projection) of these models. In Figures 1−4, we include the calculation from the SAFT-VR Mie EoS, molecular dynamics results for rings,

and also include the theory results for a chain ($\chi = 0$) fluid formed by the same number of beads, m_s. These figures quantify the importance of considering ring geometries separately; for a fixed value of m_s, eq 5 is sensitive to the geometric connectivity of the ring. Figures 3 and 4 ($m_s = 5$ and 7) are particularly revealing, as they show how even among ring molecules with the same value of m_s, their particular conformation is relevant. In general, we see that for a fixed value of m_s, the ring compounds display higher critical coordinates (i.e., temperature, pressure, and density) than the corresponding linear versions, in accordance with what is expected for common fluids, that is, compare the critical temperature of cyclooctane (647.2 K) to that n-octane (568.8 K).[28]

Corresponding States Parametrization. In order to use the proposed models for specific fluids, it is necessary to define the values of the molecular parameters χ, m_s, ε, σ, λ_r, λ_a. This can be done by using the criteria of the critical conditions of a
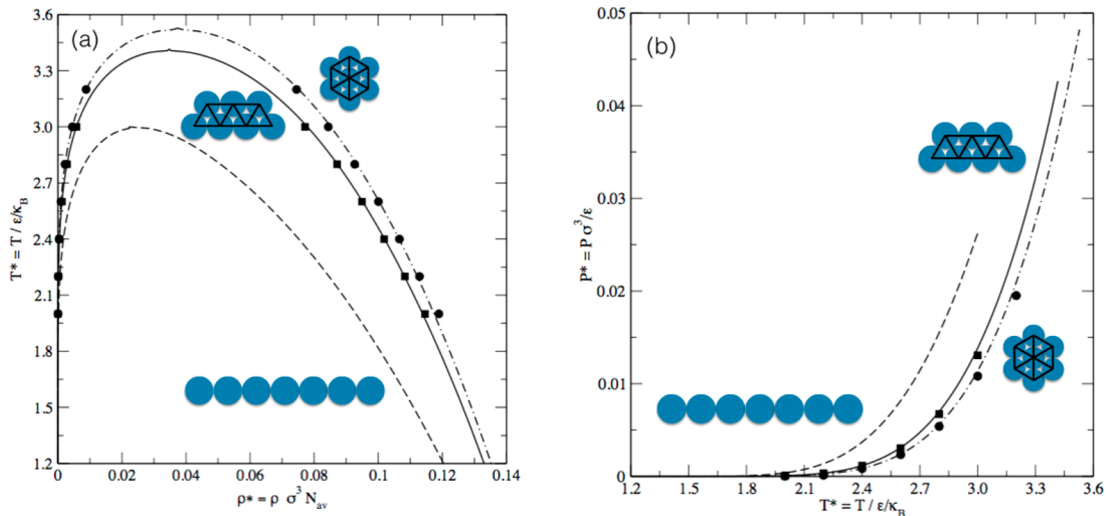
Figure 4. Phase equilibrium for $m_s = 7$: (a) coexistence densities ($\rho-T$ projection), (b) vapor pressure ($T-P$ projection). (■) MD results for geometry (f) - Table 1 ; (●) MD results for geometry (e) - Table 1 ; (—) SAFT-VR Mie EoS calculations with $\chi = 8.8640$ (geometry (f) - Table 1); (— · —) SAFT-VR Mie EoS calculations with $\chi = 9.0958$ (geometry (e) - Table 1); (- - -) SAFT-VR Mie EoS calculations with $\chi = 0$ (chain fluid).

pure fluid together with the evaluation of the liquid density at a specific condition[29] or alternatively by fitting to experimental data, for example, vapor pressure and liquid density.[10] Such an approach is exemplified in the Supporting Information by fitting the model of $m_s = 3$ (triangles) for three discotic-like molecules: benzene, hexafluorobenzene, and toluene. Alternatively, the parameters can be found by using a corresponding state parametrization. The procedure is described in detail in ref 30 and used therein to provide parameters for thousands of molecular fluids employing the linear chain approximation.[31] It will be briefly detailed here for completeness.

From the set of parameters required to describe a pure fluid, χ and m_s are predetermined according to the shape and geometric connection of molecule (see Table 1). A further reduction in the number of parameters can be made if one recognizes that, for fluid phase properties, there is an intimate relationship between the exponents λ_r and λ_a of the Mie potential, that is, their specification is not independent of each other.[32] The observation is based on the premise that the van der Waals constant, α,

$$\alpha = \frac{1}{\varepsilon \sigma^3} \int_\sigma^\infty \phi_{\text{Mie}}(r) r^2 \mathrm{d}r$$
$$= \left(\frac{\lambda_r}{\lambda_r - \lambda_a}\right)\left(\frac{\lambda_r}{\lambda_a}\right)^{\lambda_a/(\lambda_r - \lambda_a)}\left[\left(\frac{1}{\lambda_a - 3}\right) - \left(\frac{1}{\lambda_r - 3}\right)\right]$$

(6)

which captures the first order contribution to the mean field dispersion energy of the Mie potentials, establishes a unique dependence between pairs (λ_r, λ_a) of exponents, that is, fluids described by the same value of α exhibit conformal fluid phase diagrams. In that sense, for most common applications and without lack of generality, one can fix the attractive exponent λ_a to 6.0. This choice will be made here and in what follows in the manuscript $\lambda = \lambda_r$ is the only one of the Mie exponents to be fitted. The van der Waals constant is then related directly to the repulsive exponent as

$$\alpha = \frac{\lambda}{3(\lambda - 3)}\left(\frac{\lambda}{6}\right)^{6/(\lambda - 6)}$$

(7)

For each of the molecular geometries (i.e., for a given set of values of m_s and χ from Table 1) it is possible to correlate λ

with the slope of the vapor pressure curve. This is done by taking a unique point of the saturation curve at a reduced temperature of $T_r = T/T_c = 0.7$. Such point is used to define Pitzer's acentric factor, ω. Tables for the acentric factor of pure substances are commonly available, otherwise the value can be found by its definition.[33] The core of our procedure is to recognize that given the fact that we can use the SAFT-VR Mie EoS to relate macroscopic thermophysical properties with potential parameters, we can explicitly evaluate the relationship between these two conjugate properties (one microscopic and the other macroscopic) and fit the results to a Padé series

$$\lambda = \frac{\sum_{i=0} a_i \omega^i}{1 + \sum_{i=1} b_i \omega^i}$$

(8)

From the knowledge of the corresponding λ, the van der Waals constant, α, may be found from eq 7. For each possible value of α, the principle of corresponding states states that the critical properties and phase behavior can be expressed uniquely for each fluid in reduced terms, that is, scaling with respect to the appropriate energy (ε) and length (σ) scales. Thus, we express in reduced units the temperature $T^* = k_B T/\varepsilon$, as well as the density $\rho^* = \rho\sigma^3$. This unique relationship may also be expressed in parametric form if one does not desire to resolve the parent EoS. We propose the following expressions for the critical temperature T_c^*, and the reduced saturated liquid density at $T_r = 0.7$, $\rho^*|_{\text{Tr}=0.7}$

$$T_c^* = \frac{\sum_{i=0} c_i \alpha^i}{1 + \sum_{i=1} d_i \alpha^i}$$

(9)

$$\rho^*\bigg|_{T_r=0.7} = \frac{\sum_{i=0} e_i \alpha^i}{1 + \sum_{i=1} f_i \alpha^i}$$

(10)

Finally, to match the reduced behavior to that of a real fluid, we need then only two experimental points for which the corresponding values for ε and σ for a given fluid may be obtained by simple scaling

E

Table 2. Coefficients for the Eqs 8, 9, and 10 for Different Ring Configurations

geometry (a) $m_s = 3$ (0.0745 < ω < 0.7060)

i	0	1	2	3	4	5
a_i	6.9725	-24.8851	119.5032	-232.6325	177.9879	
b_i		-5.2703	22.6810	-54.7374	62.6967	-26.6382
c_i	-0.1963	3.8429	-15.5963	32.6737	-39.1147	20.9199
d_i		-5.0496	12.6694	-17.6981	11.2147	-1.1138
e_i	0.0991	-1.5927	4.6296	-4.6918	1.4552	
f_i		-9.1703	23.2400	-22.1380	6.6497	

geometry (b) $m_s = 4$ (0.1424 < ω < 0.8533)

i	0	1	2	3	4	5
a_i	6.5137	-14.8541	8.2147	2.3634		
b_i		-3.6723	4.9632	-2.7691	0.5017	
c_i	0.4901	-1.3513	-5.1730	18.0352	-13.9409	
d_i		-6.8977	15.1764	-12.8773	3.3297	-0.4160
e_i	0.1281	-1.2349	3.0728	-2.7357	0.6759	
f_i		-7.8857	18.1466	-15.3313	3.5466	

geometry (c) $m_s = 5$ (0.2061 < ω < 1.0427)

i	0	1	2	3	4	5
a_i	5.9974	-25.4418	35.1304	-8.7779	-17.4560	10.8151
b_i		-5.6278	12.6813	-14.2839	8.0207	-1.7843
c_i	-0.0574	3.1522	-14.6517	28.4219	-27.0356	10.9765
d_i		-5.0723	10.5536	-11.0175	5.3725	-0.5705
e_i	0.0975	-1.0255	3.0131	-3.6701	1.9253	-0.3682
f_i		-8.5586	23.1998	-26.9186	13.5840	-2.5091

geometry (d) $m_s = 5$ (0.2105 < ω < 0.9738)

i	0	1	2	3	4	5
a_i	5.9870	-26.3670	38.9070	-13.7206	-15.7141	11.2597
b_i		-5.7497	13.2677	-15.3524	8.8875	-2.0466
c_i	0.4786	-1.0367	-5.8418	17.9103	-13.1351	
d_i		-6.5275	13.9620	-11.7622	3.2367	-0.4277
e_i	0.1148	-1.0737	3.0574	-3.7133	1.9717	-0.3814
f_i		-8.2345	22.1442	-25.9044	13.3190	-2.4978

geometry (e) $m_s = 7$ (0.3493 < ω < 1.1271)

i	0	1	2	3	4	5
a_i	5.2601	-18.0152	21.6901	-6.0489	-6.7239	4.0247
b_i		-4.6291	8.9896	-9.0082	4.6002	-0.9466
c_i	0.4847	-0.6085	-6.8858	17.6535	-11.6816	
d_i		-5.9592	11.9474	-9.6061	2.6874	-0.3546
e_i	0.0960	-0.7875	2.1158	-2.5024	1.3246	-0.2650
f_i		-7.7202	20.0622	-23.1345	11.9742	-2.3639

geometry (f) $m_s = 7$ (0.3486 < ω < 1.1467)

i	0	1	2	3	4	5
a_i	5.3804	-19.2987	22.5961	-4.5702	-8.5162	4.4222
b_i		-4.7382	9.0450	-8.6820	4.1780	-0.8024
c_i	0.4746	-0.5674	-7.0132	17.9753	-11.9759	
d_i		-5.9993	12.1102	-9.7991	2.7465	-0.3637
e_i	0.0930	-0.7801	2.1084	-2.4943	1.3220	-0.2691
f_i		-7.8190	20.3990	-23.5642	12.2818	-2.4951

$$\varepsilon = \frac{\kappa_B T_c}{T_c^*}$$

(11)

and

$$\sigma = \left(\frac{\rho^*|_{T_r=0.7}}{\rho|_{T_r=0.7} N_{av}} \right)^{1/3}$$

(12)

Table 3. Pure Fluid Critical Temperature (T_c), Acentric Factor (ω), Liquid Density at $T_r = 0.7$ ($\rho_{Tr=0.7}$), and the Molecular Parameters ε, σ, and λ for Ring Components Discussed in This Work

fluid	T_c (K)	ω	$\rho_{Tr=0.7}$ (mol/m³)	ε/k_B (K)	σ (Å)	λ
$m_s = 3$ ($\chi = 1.4938$)						
benzene[a]	562.05	0.2092	9814.800	230.30	3.441	10.45
hexafluorobenzene[a]	516.42	0.3986	7828.647	294.23	3.772	16.53
2,5-dimethylfuran[b]	559.00	0.3191	8198.694	277.70	3.687	13.35
sulfolane[b]	855.00	0.3782	8343.743	470.27	3.685	15.58
tetrahydro-2H-pyran[b]	572.20	0.2256	8868.462	241.53	3.564	10.81
tetrahydrofuran[b]	540.20	0.2353	10920.680	232.03	3.328	11.04
toluene[a]	591.75	0.2660	8105.800	268.24	3.685	11.80
$m_s = 4$ ($\chi = 2.9833$)						
naphthalene[c]	748.33	0.3317	6547.781	281.76	3.578	11.06
pyrene[b]	938.33	0.4954	4411.178	459.04	4.134	15.79
$m_s = 5$ ($\chi = 4.7188$)						
anthracene[a]	876.00	0.3314	4875.613	259.68	3.631	9.55
$m_s = 7$ ($\chi = 9.0958$)						
coronene[a]	1143	0.6199	3907.857[d]	347.02	3.524	11.43
$m_s = 7$ ($\chi = 8.8640$)						
pentacene[b]	1079.03	0.6740	3518.840	351.68	3.664	12.48

[a]Pure fluid experimental data (T_c, ω, $\rho_{Tr=0.7}$) are taken from NIST-REFPROP database, ref 28. [b]Pure fluid experimental data (T_c, ω, $\rho_{Tr=0.7}$) are taken from DECHEMA, ref 36. [c]Pure fluid experimental data (T_c, ω, $\rho_{Tr=0.7}$) are taken from MOLInstincts, ref 34. [d]Pure fluid experimental data (T_c, ω, $\rho_{Tr=0.7}$) are calculated by using the Rackett expression.[37]
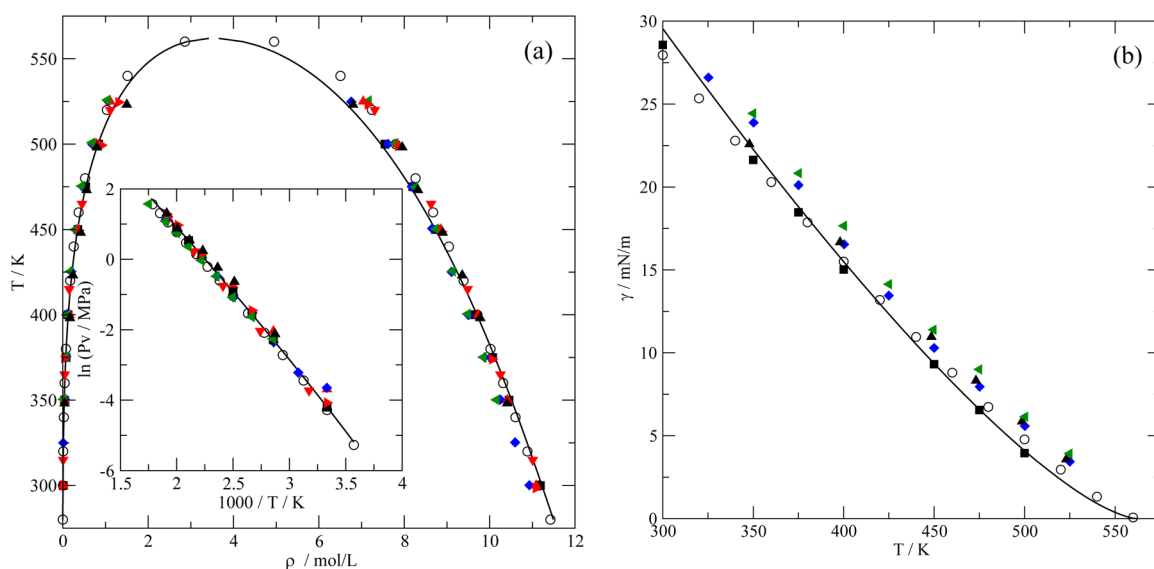

Figure 5. Phase equilibrium and interfacial tension for benzene ($m_s = 3$). (a) Coexistence densities ($\rho-T$ projection); inset: vapor pressure ($T-P$ projection). (b) Interfacial tension ($T-\gamma$ projection). (—) SAFT-VR Mie EoS calculations with $\chi = 1.4938$ and SGT with $c = 25.416 \times 10^{-20}$ J m⁵ mol⁻². (○) NIST- REFPROP database.[28] MD results: (■) this work; (left pointing, green triangle) 1 site CG;[16] (blue diamond) 3 site CG.[16] Monte Carlo simulations: (▲) 6-site TraPPE-UA;[38] (red triangle) 6 site TraPPE-UA;[23] (right pointing, red triangle) 9 site TraPPE-UA with electrostatic charges;[39] (down pointing, red triangle) 12-site TraPPE-UA-EH with electrostatic charges and explicit-hydrogen.[40]

where N_{av} is Avogadro's number.

In summary, the model relies on three molecular parameters ε, σ, and λ, which require fitting to experimental conditions. This is done by matching three chosen thermodynamic state points: the acentric factor, ω (essentially a point on the vapor pressure curve), the critical temperature, T_c, and the saturated liquid density, $\rho|_{Tr=0.7}$, at the reduced temperature $T_r = T/T_c = 0.7$, guaranteeing a good fit of the range of the potential, the energy and the length scales. In Table 2 we present the values of the parameters a_i, b_i, ..., f_i required for eqs 8−10) for each of the ring geometries discussed in Table 1 along with their range of applicability.

In the following section we illustrate the application to some representative cases, where SAFT-VR Mie is compared to MD simulations and the available reference[28,34,35] or experimental[36] data.

Application to Pure Fluids. In order to test the applicability of the proposed expression for a^{RING}, its parametrization based on corresponding state principia and the transferability of its molecular parameters from SAFT EoS model to MD simulations, we have selected some archetypal cases of ring fluids represented by $m_s = 3$, 4, 5, and 7. Table 3 summarizes the pure ring fluids tested in this work together with the values for the critical temperature (T_c), the acentric factor (ω), the liquid density at $T_r = 0.7$ ($\rho_{Tr=0.7}$) used to obtain
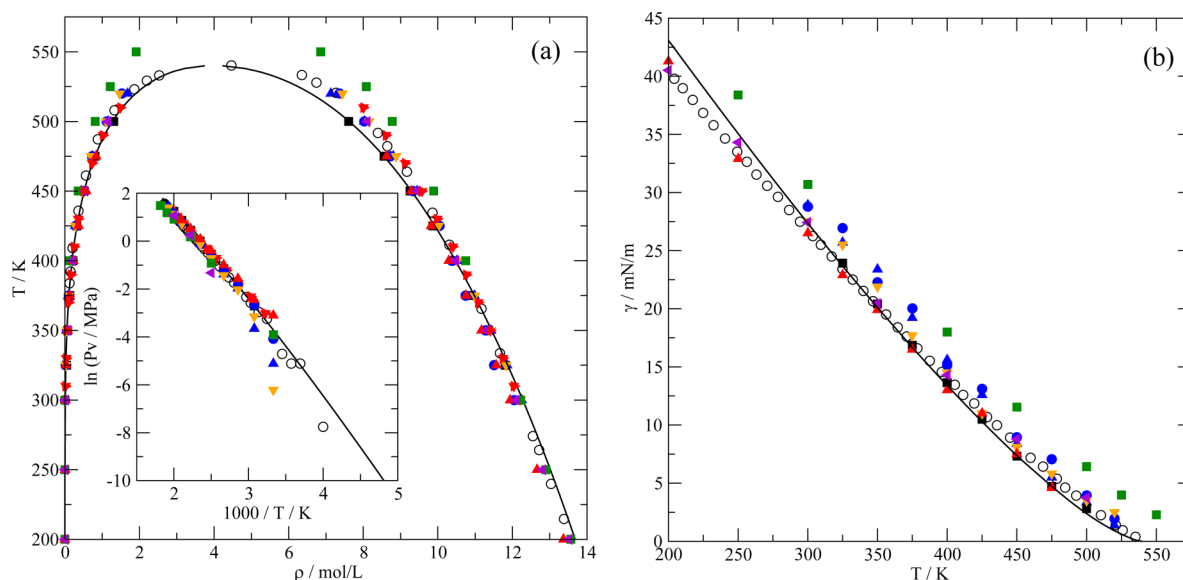
Figure 6. Phase equilibrium and interfacial tension for tetrahydrofuran ($m_s = 3$). (a) Coexistence densities ($\rho-T$ projection), inset: vapor pressure ($T-P$ projection). (b) Interfacial tension ($T-\gamma$ projection). (—) SAFT-VR Mie EoS calculations with $\chi = 1.4938$ and SGT with $c = 18.174 \times 10^{-20}$ J m^5 mol^{-2}. (○) DECHEMA database.[36] MD results: (■) this work; (blue circle) 1-site CG;[41] (down pointing, yellow triangle) 2-site CG;[41] (blue triangle) 3-site CG;[41] (green square) 5-site Jorgensen-UA;[41] (red triangle) 5-site Rigid-UA;[41] (left pointing, purple triangle) 5-site TraPPE-UA;[41] Monte Carlo simulations: (right pointing, red triangle) 5-site TraPPE-UA;[40] (down pointing, red triangle) 5-site TraPPE-UA with electrostatic charges.[42]
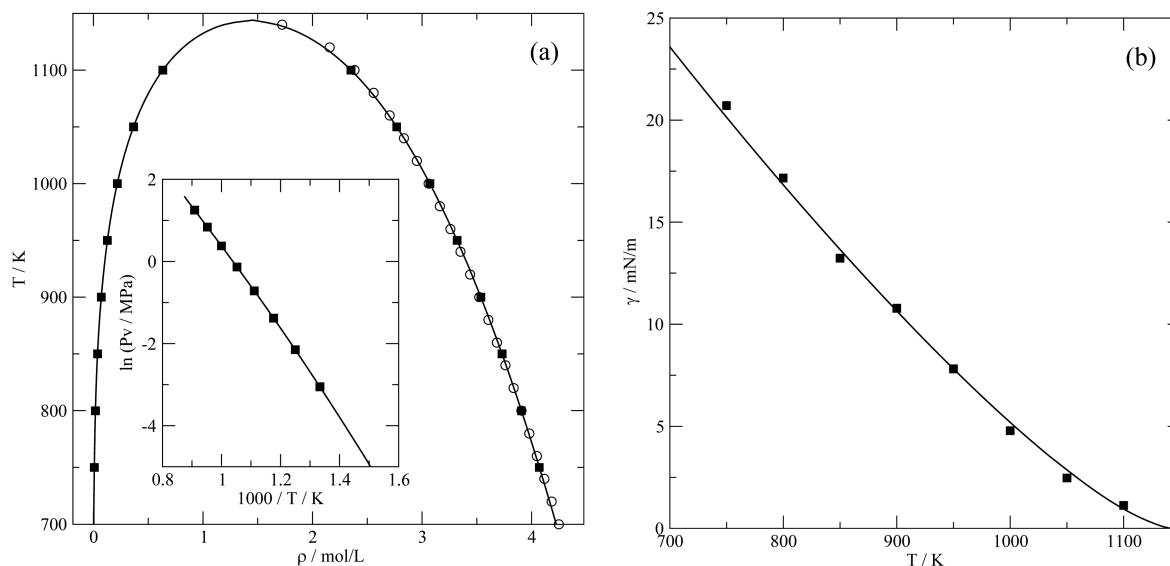

Figure 7. Predicted phase equilibrium and interfacial tension for coronene ($m_s = 7$). (a) Coexistence densities ($\rho-T$ projection); inset: vapor pressure ($T-P$ projection). (b) Interfacial tension ($T-\gamma$ projection). (—) SAFT-VR Mie EoS calculations with $\chi = 9.0958$ and SGT with $c = 125.898 \times 10^{-20}$ J m^5 mol^{-2}. (■) this work; (○) Reference data for ρ^L have been estimated from Rackett.[37]

the corresponding molecular parameters m_s, ε, σ, and λ from the correlations (eqs 8-10).

The molecular parameters listed in Table 3 have been simultaneously used in both the SAFT EoS model and MD simulations to carry out phase equilibria and interfacial properties calculations. Selected numerical values obtained from MD simulations presented in Table 3 are included in the Supporting Information. The corresponding statistical deviations of the results presented here and those obtained from other authors have been summarized in Table S19 (Supporting Information). These values are obtained from the comparison between molecular simulation and the reference or experimental data. The quoted figures also include the reference or experimental data reported in databases such as NIST-REFPROP[28] and DECHEMA,[36] and reported results are from molecular simulations that employ other molecular models (e.g., CG or united atom force fields). The SAFT EoS calculations and MD simulation agree with each other to within a deviation of 1% for phase equilibria predictions. Table S19 also includes the error observed when comparing the interfacial tension between the liquid and vapor bulk phases calculated from MD by employing the virial route against the experimental information. Interfacial tensions are not an input to the fitting of the potential or the EoS and provide a sensitive gauge to the quality and consistency of the density predictions obtained from the force fields.

While the tables are too lengthy to discuss in detail, we selected two representative triangle fluids and compare the results graphically. Figure 5 and 6 show the comparisons for benzene, and tetrahydrofuran. Benzene and tetrahydrofuran are particularly relevant, as both have been previously modeled both as fully atomistic models, united atom representations where the hydrogens are lumped into the descriptions of the heavy atoms and as CG three-bead (equilateral triangle configuration) employing a related top-down approach through the use of fitting via the SAFT-VR Mie.[16,41] The high-fidelity models[23,39−41] are computationally much more expensive and do not provide any further level of accuracy,[23,39−41] exception being the fully atomistic TraPPE-UA-EH[40] model of benzene.

For the case of previous models of ring fluids fitted using the SAFT top-down methodology,[16,41] as these did not employ the appropriate form of the EoS, the molecular parameters obtained by fitting the EoS to experimental data had to be further refined (scaled) in order for the simulations to match experimental data, limiting the predictive nature of the procedure.

For the case of naphtalene and anthracene, the CG for models for rings display low ADDs in density and vapor pressure (data in the Supporting Information) . For the other fluids presented in Tables 3, this work represents predictions of the hypothetical phase equilibria, as the temperatures will most likely be above the decomposition temperatures for these organic fluids. Example is given in Figure 7 with the presumed phase equilibria of coronene.

Besides the phase equilibrium, Table S19 includes a comparison of the accuracy of the calculation of the interfacial tension, obtained through the Square Gradient Theory (details in the Supporting Information), showcasing the accuracy and predictive nature of the model. Figure 8 displays the density profiles across a vapor−liquid interface, $\rho(z)$, profiles computed both from the theory and MD simulations at three temperatures for benzene. The classical hyperbolic profiles described
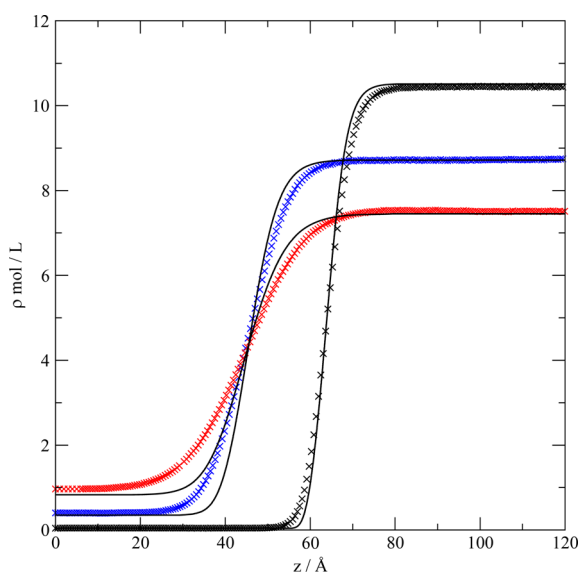
by the theory agree with the MD results, and as expected, the interfacial width increases with temperature.

Applications to Mixtures. The extension of the model for the case of fluid mixtures is straightforward, as the eq 5 reverts to the case of a linear chain when $\chi = 0$. For mixtures (which may include linear chains, rings or both) it is necessary to replace the original contribution of a^{CHAIN} for the following expression, which accounts for both chain and ring fluids:

$$a^{RING} = -\sum_{i=1}^{n_c} x_i(m_{si} - 1 + \chi_i\eta_i)\ln[g_{ii}^{Mie}(\sigma)] \tag{13}$$

where the subscript i runs over all the individual n_c components (not beads) in the mixture. As the other terms in the perturbation expansion (eq 1) remain unchanged, the methodology to solve phase equilibria and obtain thermophysical properties remain unchanged with respect to the original versions of the EoS. In particular, for a mixture, one must define combinations rules to be used both in the simulations and within the theory. We employ the same choice originally suggested by Lafitte et al.,[10]

$$\sigma_{ij} = \frac{\sigma_{ii} + \sigma_{jj}}{2}; \quad \varepsilon_{ij} = (1 - k_{ij})\frac{\sqrt{\sigma_{ii}^3\sigma_{jj}^3}}{\sigma_{ij}^3}\sqrt{\varepsilon_{ii}\varepsilon_{jj}};$$

$$(\lambda_{ij} - 3)^2 = (\lambda_{ii} - 3)(\lambda_{jj} - 3) \tag{14}$$

There is no expectation that the mixture behavior will match these idealized results, hence, a binary interaction parameter, k_{ij}, is included in the cross energy term. This interaction parameter can be obtained from experimental data.

To illustrate the performance of this extension for fluid mixtures, we consider the binary mixture composed by hexane and tetrahydro-2H-pyran (THP). For this application, hexane is modeled as chain fluid formed by two tangential spheres, $m_s = 2$ with parameters taken from the literature,[43] $\sigma = 4.508$ Å, $\varepsilon/k_B = 376.35$ K, $\lambda = 19.57$, whereas THP is modeled as an equilateral triangle with $m_s = 3$ with parameters taken from Table 3.

Figure 9a displays the vapor−liquid phase equilibria (VLE) at 94 kPa, while Figure 9b displays the phase equilibria in a temperature−mass density diagram. The theory is resolved using a value of $k_{ij} = -0.022$, which is obtained from the fitting of the EoS model to the experimental data.[44] Details of the calculation of the equilibria are given in the Supporting Information. The SAFT model correctly accounts for the zeotropic behavior of this mixture in the whole mole fraction range with a low absolute average deviation in boiling temperature (0.05%) and vapor mole fraction (0.91%.). While arguably such a quality of fit could be obtained by employing other versions of SAFT (and indeed other EoS), Figure 9 also includes the results obtained from performing molecular dynamics simulations using the same molecular parameters employed in the theory. The agreement between the theory and the simulations is unique to this treatment. Simulation details and numerical results are provided in the Supporting Information (see Tables S14 and S15).

A further test is the prediction of the homogeneous liquid density of the mixture at isothermal−isobaric conditions. Figure 10 displays the mass liquid density as a function of the mole fraction of the mixture at 298.15 K and 101.325 kPa (numerical data are presented in Table S16 of the Supporting Information) including also the SAFT calculations with $k_{ij} = -0.022$ and MD
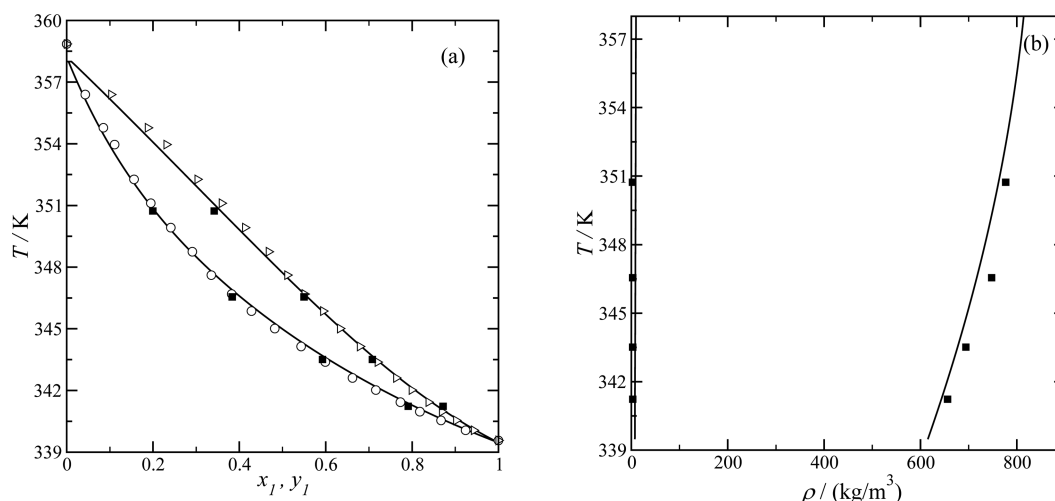

Figure 8. Density profiles $\rho(z)$ across the vapor−liquid interface for benzene. (—) SAFT-VR Mie EoS calculations with $\chi = 1.4938$ and SGT with $c = 25.416 \times 10^{-20}$ J m^5 mol^{-2}. (×) MD results at (black) $T = 350$ K; (blue) $T = 450$ K; (red) 500 K.

Figure 9. Phase equilibrium for hexane (1) + THP (2) at 94 kPa. (a) Boiling temperature (T) as a function of the liquid (x_1) and vapor (y_1) mole fractions; (b) Boiling temperature (T) as a function of the bulk mass densities for the liquid (ρ^L) and vapor (ρ^V) phases. (—) SAFT-VR Mie EoS calculations with $k_{ij} = -0.022$; (○) Experimental data from Mejía et al.;[44] (■) MD from this work (see numerical values in Table S15 of Supporting Information).
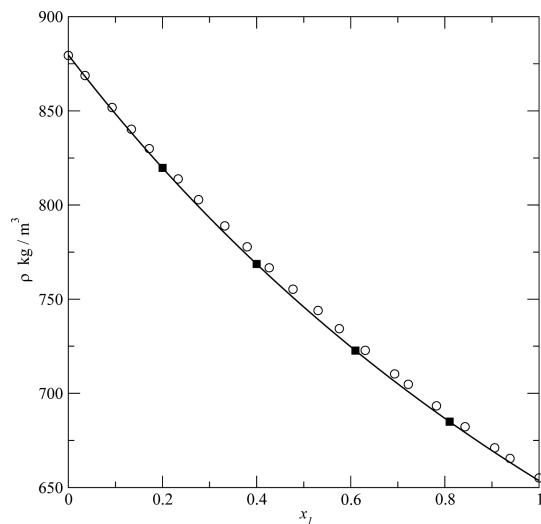

Figure 10. Liquid density as a function of the liquid (x_1) mole fraction for hexane (1) + THP (2) at 298.15 K and 101.325 kPa. (—) SAFT-VR Mie EoS calculations with $k_{ij} = -0.022$; (○) Experimental data from this work (see numerical values in Table S20 of Supporting Information); (■) MD from this work (see numerical values in Table S16 of Supporting Information).

results. There is an absolute average deviation (AAD) of 0.41% for the SAFT calculations and 0.49% for the MD results.

■ CONCLUSIONS

We present a modification to the SAFT-VR Mie EoS that allows the accurate representation of the properties of planar rings. Specific expressions for use in the case of rings composed of 3, 4, 5 (two configurations) and 7 (two configurations) beads are given in terms of a unique fixed parameter χ. Further expressions are provided that allow the parametrization of the EoS invoking the corresponding states principle. This approach provides molecular parameters from the knowledge of three state points: the critical temperature, acentric factor, and a reference liquid density of the pure fluid. The proposed approach has been tested by predicting the phase equilibria for discotic molecules and mixture of discotic and linear molecules

and, when available, compared to experimental data. An important aspect of the proposed model is the direct link that exists between the molecular parameters underlying the Hamiltonian that defines the theory and the molecular simulations that employ the same parameters. This correspondence provides evidence that the approximations made within the theory are robust and accurate. The parallelism between the theory and the simulation models becomes important when dealing with interfacial and transport properties, where the theoretical developments are less refined. As an example, in Table S15 of the Supporting Information we present the results of the interfacial tension for a heptane−THP mixture where, as expected, the tension decreases as temperature and/or mole fraction increases, and while no isobaric experimental data is available to compare to, we have enough confidence in the models to trust these results.[45] In essence, the procedure of fitting molecular EoS parameters to experimental data becomes a shortcut to parametrize force fields for molecular simulations, with the advantage of producing effective pairwise intermolecular potentials which are fitted not to a few properties, but to provide the best compromise fit of the full free energy landscape. Comparison of structural and transport properties, such as radial distribution functions, diffusion, shear viscosity, and thermal conductivity are beyond the scope of this manuscript, although there are indications[16,41] that suggest a similar level of accuracy.

■ APPENDIX

Following the second order thermodynamic theory (TPT2) for hard spheres as proposed initially by Wertheim,[21] one can express the compressibility factor $Z = P/\rho k_B T$ of a hard sphere chain of m_s spherical segments by

$$Z = Z_{ref} + Z_1 + Z_2 \tag{A.1}$$

where Z_{ref} is the reference term for hard spheres, Z_1 and Z_2 correspond to the first and second-order terms in the perturbation series, respectively, P, T, and ρ correspond to the pressure, temperature and molecular number density, respectively. In order to produce a closed expression for the reference and first-order terms of the Z expansion, one can

adopt the Carnahan−Starling expression[46] for Z_{ref} and a value of $g_{HS}(\sigma)$ consistent with it for the Z_1 and Z_2 terms. For specific details the reader is referred to refs 20 and 21.

The final forms of Z_{ref}, Z_1, and Z_2 are given by the following expressions:

$$Z_{ref} = m_s \left[\frac{1 + \eta + \eta - \eta^2}{(1 - \eta)^3} \right] \tag{A.2}$$

$$Z_1 = -(m_s - 1)\left[\frac{2 + 2\eta - \eta^2}{(2 - \eta)(1 - \eta)} \right] \tag{A.3}$$

$$Z_2 = \frac{4s - m_s(1 + 4s)[m_s^2(1 + 4s) - 4s]^{1/2}}{2s(1 + 4s)}\left(\eta \frac{\partial s}{\partial \eta} \right) \tag{A.4}$$

In eqs A.2−A.4, η represents the packing factor, $\eta = m_s \pi \rho \sigma^3 / 6$, where ρ is the number density of molecules, and σ is the diameter of a single sphere (monomer). For a fixed bond angle θ, the parameter s is given by

$$s = \left\{ \frac{g_{HS}^{(3)}[\sigma, \sigma, 2\sigma \sin(\theta/2)]}{g_{HS}(\sigma)^2} - 1 \right\} \tag{A.5}$$

In eq A.5, $g_{HS}(\sigma)$ is the contact value of the radial distribution function for hard spheres, and $g_{HS}^{(3)}$, is the triplet correlation function of three touching hard spheres. Müller and Gubbins[47] evaluated this latter quantity and provided[21] a closed form expression for $g_{HS}^{(3)}$, which for the case of an equilateral triangle, $\theta = 60°$, becomes

$$g_{HS}^{(3)}[\sigma, \sigma, \sigma] = g_{HS}(\sigma)^2 \left\{ \frac{1 - 1.7568\eta + 1.5779\eta^2}{(1 - \eta^3)} \right\} \tag{A.6}$$

Since for the case of $m_s = 3$, $\theta = 60°$ TPT2 will provide an exact result for ring molecules with an equilateral triangle conformation (Model a, Table 1), it is illustrating to equate the compressibility factor obtained from TPT2 result (eqs A.1−A.6 evaluated at $m_s = 3$) to that obtained from the more common TPT1 formulation (eqs A.1 and A.2 evaluated at m_{eff}) in order to back calculate an "effective" value of number of segments, m_{eff}, that will produce the correct result,

$$(m_{eff} - m_s)\left[\frac{2 + 2\eta - \eta^2}{(2 - \eta)(1 - \eta)} \right]$$
$$= \frac{4s - m_s(1 + 4s)[m_s^2(1 + 4s) - 4s]^{1/2}}{2s(1 + 4s)}\left(\eta \frac{\partial s}{\partial \eta} \right) \tag{A.7}$$

Inexorably, the result is density dependent and may be expressed in a simplified form as $m_{eff} = m_s - 1 + 1.3287\eta$ (see Supporting Information). While this is an exact result for hard sphere triangles, we make the assumption that it may be used equally for other potentials, adopting it to SAFT-VR Mie EoS and thus providing an expression for the ring contribution within TPT1, namely, eq 5.

■ ASSOCIATED CONTENT

ⓢ Supporting Information

The Supporting Information is available free of charge on the ACS Publications website at DOI: 10.1021/acs.langmuir.7b00976.

Molecular simulations details and numerical results; Experimental details and results; Methodologies for evaluation of phase equilibria and interfacial tensions; Additional comparisons of the agreement between theory and simulations (PDF).

■ AUTHOR INFORMATION

Corresponding Author
*E-mail: amejia@udec.cl.

ORCID ⓘ
Erich A. Müller: 0000-0002-1513-6686
Andrés Mejía: 0000-0001-7238-6633

Notes
The authors declare no competing financial interest.

■ ACKNOWLEDGMENTS

■ REFERENCES

(1) Wertheim, M. S. Fluids with highly directional attractive forces. I. Statistical thermodynamics. *J. Stat. Phys.* **1984**, *35*, 19−34.

(2) Wertheim, M. S. Fluids with highly directional attractive forces. II. Thermodynamic perturbation theory and integral equations. *J. Stat. Phys.* **1984**, *35*, 35−47.

(3) Wertheim, M. S. Fluids with highly directional attractive forces. III. Multiple attraction sites. *J. Stat. Phys.* **1986**, *42*, 459−476.

(4) Wertheim, M. S. Fluids with highly directional attractive forces. IV. Equilibrium polymerization. *J. Stat. Phys.* **1986**, *42*, 477−492.

(5) Müller, E. A.; Gubbins, K. E. Molecular-based equations of state for associating fluids: A review of SAFT and related approaches. *Ind. Eng. Chem. Res.* **2001**, *40*, 2193−2211.

(6) Economou, I. G. Statistical associating fluid theory: A successful model for the calculation of thermodynamic and phase equilibrium properties of complex fluid mixtures. *Ind. Eng. Chem. Res.* **2002**, *41*, 953−962.

(7) Tan, S. P.; Adidharma, H.; Radosz, M. Recent advances and applications of statistical associating fluid theory. *Ind. Eng. Chem. Res.* **2008**, *47*, 8063−8082.

(8) McCabe, C.; Galindo, A. SAFT associating fluids and fluid mixtures. In *Applied Thermodynamics of Fluids*; Goodwin, A., Sengers, J. V., Peters, C. J., Eds; Royal Society of Chemistry: London, 2010; Chapter 8.

(9) Kontogeorgis, G. M.; Folas, G. K. *Thermodynamic Models for Industrial Applications: From Classical and Advanced Mixing Rules to Association Theories*; Wiley-Blackwell, 2010.

(10) Lafitte, T.; Apostolakou, A.; Avendaño, C.; Galindo, A.; Adjiman, C. S.; Müller, E. A.; Jackson, G. Accurate statistical associating fluid theory for chain molecules formed from Mie segments. *J. Chem. Phys.* **2013**, *139*, 154504.

(11) Zhou, S.; Solana, J. R. Progress in the Perturbation Approach in Fluid and Fluid-Related Theories. *Chem. Rev.* **2009**, *109*, 2829−2858.

(12) Mie, G. Zur kinetischen Theorie der einatomigen Körper. *Ann. Phys.* **1903**, *316*, 657−697 The Mie potential actually predated the

Lennard-Jones form. See the introduction of ref 10 for a discussion of the history of modern intermolecular potentials..

(13) Müller, E. A.; Jackson, G. Force field parameters from the SAFT-γ equation of state for use in Coarse-Grained Molecular Simulations. *Annu. Rev. Chem. Biomol. Eng.* **2014**, *5*, 405−427.

(14) Avendaño, C.; Lafitte, T.; Galindo, A.; Adjiman, C. S.; Jackson, G.; Müller, E. A. SAFT-γ force field for the simulation of molecular fluids. 1. A single-site coarse grained model of carbon dioxide. *J. Phys. Chem. B* **2011**, *115*, 11154−11169.

(15) Avendaño, C.; Lafitte, T.; Adjiman, C. S.; Galindo, A.; Müller, E. A.; Jackson, G. SAFT-γ force field for the simulation of molecular fluids: 2. Coarse-grained models of greenhouse gases, refrigerants, and long alkanes. *J. Phys. Chem. B* **2013**, *117*, 2717−2733.

(16) Lafitte, T.; Avendaño, C.; Papaioannou, V.; Galindo, A.; Adjiman, C. S.; Jackson, G.; Müller, E. A. SAFT-γ force field for the simulation of molecular fluids: 3. Coarse-grained models of benzene and hetero-group models of n-decylbenzene. *Mol. Phys.* **2012**, *110*, 1189−1203.

(17) Mejía, A.; Cartes, M.; Segura, H.; Müller, E. A. Use of equations of state and coarse grained simulations to complement experiments: describing the interfacial properties of carbon dioxide + decane and carbon dioxide + eicosane mixtures. *J. Chem. Eng. Data* **2014**, *59*, 2928−2941.

(18) Cumicheo, C.; Cartes, M.; Segura, H.; Müller, E. A.; Mejía, A. High-pressure densities and interfacial tensions of binary systems containing carbon dioxide + n-alkanes: (n-dodecane, n-tridecane, n-tetradecane). *Fluid Phase Equilib.* **2014**, *380*, 82−92.

(19) Lobanova, O.; Avendaño, C.; Lafitte, T.; Jackson, G.; Müller, E. A. SAFT-γ Force Field for the Simulation of Molecular Fluids. 4. A Single- Site Coarse Grained Model of Water Valid Over a Wide Temperature Range. *Mol. Phys.* **2015**, *113*, 1228−1249.

(20) Müller, E. A.; Gubbins, K. E. Simulation of hard triatomic and tetratomic molecules. A test of associating fluid theory. *Mol. Phys.* **1993**, *80*, 957−976.

(21) Wertheim, M. S. Thermodynamic perturbation theory of polymerization. *J. Chem. Phys.* **1987**, *87*, 7323−7331.

(22) Sear, R. P.; Jackson, G. Theory and computer simulation of hard-sphere models of ring molecules. *Mol. Phys.* **1994**, *81*, 801−811.

(23) Wick, C. D.; Martin, M. G.; Siepmann, J. I. Transferable potentials for phase equilibria. 4. United-atom description of linear and branched alkenes and of alkylbenzenes. *J. Phys. Chem. B* **2000**, *104*, 8008−8016.

(24) Haghmoradi, A.; Wang, L.; Chapman, W. G. A new equation of state for associating Lennard−Jones fluids with two sites: small bond angle. *Mol. Phys.* **2016**, *114*, 2548−2557.

(25) Huang, S. H.; Radosz, M. Equation of State for Small, Large, Polydisperse, and Associating Molecules. *Ind. Eng. Chem. Res.* **1990**, *29*, 2284−2294.

(26) Sear, R. P.; Jackson, G. Thermodynamic perturbation theory for association into chains and rings. *Phys. Rev. E* **1994**, *50*, 386−394.

(27) Sear, R. P.; Jackson, G. The ring integral in a thermodynamic perturbation theory for association. *Mol. Phys.* **1996**, *87*, 517−521.

(28) Lemmon, E. W.; McLinden, M. O.; Friend, D. G. Thermophysical Properties of Fluid Systems in NIST Chemistry WebBook, NIST Standard Reference Database Number 69; Linstrom, P. J., Mallard, W. G., Eds.; National Institute of Standards and Technology: Gaithersburg MD, http://webbook.nist.gov; retrieved Feb, 2017.

(29) Polishuk, I. Standardized Critical Point-Based Numerical Solution of Statistical Association Fluid Theory Parameters: The Perturbed Chain-Statistical Association Fluid Theory Equation of State Revisited. *Ind. Eng. Chem. Res.* **2014**, *53*, 14127−14141.

(30) Mejía, A.; Herdes, C.; Müller, E. A. Force Fields for Coarse-Grained Molecular Simulations from a Corresponding States Correlation. *Ind. Eng. Chem. Res.* **2014**, *53*, 4131−4141.

(31) Ervik, Å.; Mejía, A.; Muller, E. A. Bottled SAFT: a web app providing SAFT-γ Mie force field parameters for thousands of molecular fluids. *J. Chem. Inf. Model.* **2016**, *56*, 1609−1614.

(32) Ramrattan, N. S.; Avendaño, C.; Müller, E. A.; Galindo, A. A corresponding-states framework for the description of the Mie family of intermolecular potentials. *Mol. Phys.* **2015**, *113*, 932−947.

(33) Pitzer, K. S.; Lippmann, D. Z.; Curl, R. F.; Huggins, C. M.; Petersen, D. E. The Volumetric and Thermodynamic Properties of Fluids. II. Compressibility Factor, Vapor Pressure and Entropy of Vaporization 1. *J. Am. Chem. Soc.* **1955**, *77*, 3433−3440.

(34) MOLInstincts, http://search.molinstincts.com/properties/ (retrieved Feb, 2017).

(35) Daubert, E.; Danner, R. P.; Sibul, H. M.; Stebbins, C. C. *Physical and Thermodynamic Properties of Pure Chemicals. Data Compilations*; Taylor & Francis: Bristol, 1989−2002.

(36) DECHEMA Gesellschaft für Chemische Technik und Biotechnologie e.V., Frankfurt am Main, Germany http://detherm. cds.rsc.org/detherm/detherm.php (retrieved Aug, 2016).

(37) Rackett, H. G. Equation of State for Saturated Liquids. *J. Chem. Eng. Data* **1970**, *15*, 514−517.

(38) Janecek, J.; Krienke, H.; Schmeer, G. Inhomogeneous Monte Carlo simulation of the vapor-liquid equilibrium of benzene between 300 and 530 K. *Condens. Matter Phys.* **2007**, *10*, 415−423.

(39) Wick, C. D.; Siepmann, J. I.; Klotz, W. L.; Schure, M. R. Temperature effects on the retention of n-alkanes and arenes in helium-squalane gas-liquid chromatography: Experiment and molecular simulation. *J. Chromatogr. A* **2002**, *954*, 181−190.

(40) Rai, N.; Siepmann, J. I. Transferable potentials for phase equilibria. 9. Explicit-hydrogen description of benzene and 5-membered and 6-membered heterocyclic aromatic compounds. *J. Phys. Chem. B* **2007**, *111*, 10790−10799.

(41) Garrido, J. M.; Algaba, J.; Míguez, J. M.; Mendiboure, B.; Moreno-Ventas Bravo, A. I.; Piñeiro, M. M.; Blas, F. J. On interfacial properties of tetrahydrofuran: Atomistic and coarse-grained models from molecular dynamics simulation. *J. Chem. Phys.* **2016**, *144*, 144702.

(42) Keasler, S. J.; Charan, S. M.; Wick, C. D.; Economou, I. G.; Siepmann, J. I. Transferable Potentials for Phase Equilibria−United Atom. Description of Five- and Six-Membered Cyclic Alkanes and Ethers. *J. Phys. Chem. B* **2012**, *116*, 11234−11246.

(43) Herdes, C.; Totton, T. S.; Müller, E. A. Coarse grained force field for the molecular simulation of natural gases and condensates. *Fluid Phase Equilib.* **2015**, *406*, 91−100.

(44) Mejía, A.; Segura, H.; Cartes, M.; Pérez-Correa, J. R. Experimental determination and theoretical modeling of the vapor−liquid equilibrium and surface tensions of hexane + tetrahydro-2H-pyran. *Fluid Phase Equilib.* **2012**, *316*, 55−65.

(45) The use of the potentials described herein allowed a team to win the ninth industrial fluid properties simulation challenge, predicting the interfacial tension of a toluene/dodecane/water mixture surpassing the accuracy of other traditional quantum, atomistic, and theory approaches (www.fluidproperties.org); Accessed 28 Feb 2017.

(46) Carnahan, N. E.; Starling, K. E. Equation of State for Nonattracting Rigid Spheres. *J. Chem. Phys.* **1969**, *51*, 635−636.

(47) Müller, E. A.; Gubbins, K. E. Triplet correlation-function for hard-sphere systems. *Mol. Phys.* **1993**, *80*, 91−101.

■ NOTE ADDED AFTER ASAP PUBLICATION

This paper was published ASAP on June 28, 2017, with production errors in equations 6, 13, and A.3. The corrected version was reposted on June 29, 2017.